

Direct Acceleration of Electrons in a Corrugated Plasma Waveguide

A. G. York* and H. M. Milchberg

Institute for Physical Science and Technology, University of Maryland, College Park, Maryland 20742, USA

J. P. Palastro and T. M. Antonsen

Institute for Research in Electronics and Applied Physics, University of Maryland, College Park, Maryland 20742, USA

(Received 15 August 2007; published 14 May 2008)

Historically, direct acceleration of charged particles by electromagnetic fields has been limited by diffraction, phase matching, and material damage thresholds. A recently developed plasma micro-optic [B. Layer *et al.*, Phys. Rev. Lett. **99**, 035001 (2007)] removes these limitations and promises to allow high-field acceleration of electrons over many centimeters using relatively small femtosecond lasers. We present simulations that show a laser pulse power of 1.9 TW should allow an acceleration gradient larger than 80 MV/cm. A modest power of only 30 GW would still allow acceleration gradients in excess of 10 MV/cm.

DOI: 10.1103/PhysRevLett.100.195001

PACS numbers: 52.38.Kd, 41.75.Jv, 41.75.Lx, 52.50.Jm

Laser wakefield acceleration [1] of electrons to relativistic velocities is often described as a “tabletop” technology, promising to make high-energy electrons accessible to small labs and hospitals. Wakefield acceleration, however, typically requires multi-terawatt laser systems that literally stretch the definition of “table.” Direct laser acceleration [2] offers an attractive alternative for producing fast electrons. Unlike wakefield acceleration, direct laser acceleration is a linear process with no threshold intensity. Typical few-mJ chirped-pulse regenerative amplifiers that could never reach the intensity threshold for wakefield acceleration could still be used for direct laser acceleration.

A wide variety of arrangements have been used to enable the exchange of energy between radiation and relativistic electrons, from a multi-kilometer-long microwave-frequency copper waveguide [3], to a hydrogen gas irradiated by a conically-focused, radially-polarized CO₂ laser [4], to a metal tape positioned at the focus of a picosecond laser [5]. While the efficiency and expense of these schemes varies greatly, the electron acceleration gradients they can achieve are ultimately limited by the field strength they can produce and control, typically less than 1 MV/cm. Modern femtosecond lasers based on chirped-pulse amplification [6] can produce focused field strengths in excess of 10 GV/cm. An accelerating structure which could control such fields would allow enormous acceleration gradients, but no material can survive this intensity unionized. We therefore consider an accelerating structure which is already ionized: the recently demonstrated corrugated plasma waveguide [7], described in Fig. 1. We show that in this structure, a laser pulse power of 1.9 TW gives an acceleration gradient of 84 MV/cm, and only 30 GW still gives an acceleration gradient of 10.6 MV/cm.

The use of uncorrugated plasma waveguides [8] for direct electromagnetic acceleration has been suggested by Serafim *et al.* [9], who proposed guiding a radially polarized laser pulse to accelerate a copropagating relativistic electron bunch. The laser’s dominant radial compo-

nent E_r guides as a hollow mode with peak intensity at $r = w_{\text{ch}}/\sqrt{2}$, where the mode radius w_{ch} is given by $w_{\text{ch}} = (1/\pi r_e \Delta N_e)^{1/2}$, r_e is the classical electron radius and ΔN_e is the electron density difference between $r = 0$ and $r = w_{\text{ch}}$. The accelerating field is the associated axial component E_z , which peaks at $r = 0$ and passes through zero at $r = w_{\text{ch}}$. Following reference [9], the peak axial acceleration gradient from hollow beam guiding in a plasma channel is given by E [GV/cm] = $98\lambda P^{1/2}/w_{\text{ch}}^2$, where λ (laser wavelength) and w_{ch} are in μm , and P is the peak laser power in TW. For a 1.9 TW laser pulse with $\lambda = 800$ nm in a channel supporting $w_{\text{ch}} = 15 \mu\text{m}$, E_z is an

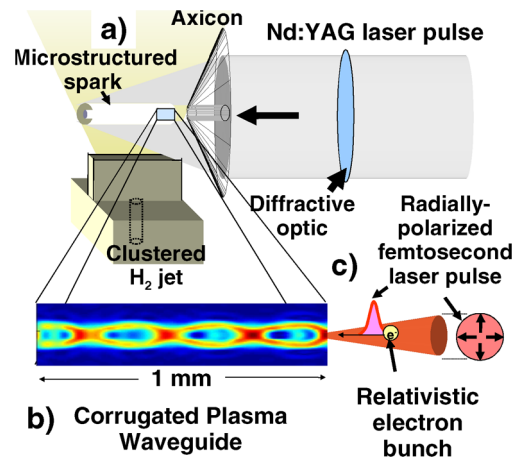


FIG. 1 (color online). Direct acceleration of electrons by a femtosecond laser pulse in a corrugated plasma waveguide. (a) A radially-modulated Nd:YAG laser pulse focused by an axicon onto a gas jet creates a spark several centimeters long with micron-scale structure. Over nanoseconds, this spark expands into (b) a hollow optical waveguide with corrugations in the guiding direction, allowing fine velocity control of guided radiation [7]. (c) A radially polarized femtosecond laser pulse and a relativistic electron bunch are injected into this waveguide. If the corrugation period is matched to L_d , the laser pulse can accelerate these electrons.

impressive 0.49 GV/cm. If there were no slippage between the laser phase velocity and the electron velocity (essentially c), this would compare very favorably to laser wakefield acceleration: Malka *et al.* used a 30 TW laser to produce an acceleration gradient of 0.66 GV/cm (200 MV over 3 mm) [1]. A regenerative amplifier with 1 mJ output can easily produce 20 GW peak power, giving a 49 MV/cm gradient. Of course, a means must be found to slow the laser phase velocity to c or less to match the relativistic electron velocity. Neutral gas as proposed in [9] will not survive the laser intensities essential for high values of accelerating field E_z ; even pulses well below the terawatt level will propagate in fully ionized waveguides. Without neutral gas, the laser phase velocity in an uncorrugated plasma waveguide is strictly superluminal: a relativistic electron would slip 2π out of phase with the accelerating pulse after propagating a dephasing length $L_d = \lambda(N_0/N_{cr} + 2\lambda^2/\pi^2 w_{ch}^2)^{-1}$ [10], where N_0 is the on-axis plasma electron density of the channel and N_{cr} is the critical plasma density. The electron receives no net acceleration: acceleration over $L_d/2$ would be cancelled by deceleration over the next $L_d/2$.

The corrugated plasma waveguide shown in Fig. 1(b) can quasi-phasesmatch (QPM) this interaction. Laser phase velocity is locally faster in high plasma-density regions and slower in low plasma density. If L_d and the corrugation period are matched, the symmetry between acceleration and deceleration in a dephasing cycle is broken, and a properly phased electron will gain net energy; this process can be viewed as the inverse of transition radiation [11].

We obtain physical insight into the QPM process from finite-difference time-domain simulations of linear pulse propagation in the simplified plasma density shown in Fig. 2(a). This simulation performed using a freely available software package with subpixel smoothing for increased accuracy [12] assumes cylindrical symmetry, and includes plasma dispersion, finite pulse duration, and pulse leakage out of the channel. Finite computing resources force us to use an unrealistically long wavelength of $6.4 \mu\text{m}$, so the waveguide density was scaled to make the laser phase velocity comparable to experimental conditions. Figure 2(b) shows the relative longitudinal and 2(c) the transverse electric field (scaled for visibility) felt by a relativistic ($v_z = c$) electron copropagating with the laser pulse nearly on axis. The channel's corrugation period is matched to L_d , and the initial phase between the electron and the laser field is chosen so that the electron is accelerated in the low-density section of each corrugation. Phase velocity is lower in these regions, so dephasing is slower and the electron spends more than half of each L_d in phase with the accelerating field. Each oscillation in 2(b) represents one dephasing cycle, and the number at each half-cycle is proportional to the energy gained or lost by the electron in that region. The electron clearly gains more energy during acceleration than it loses during deceleration.

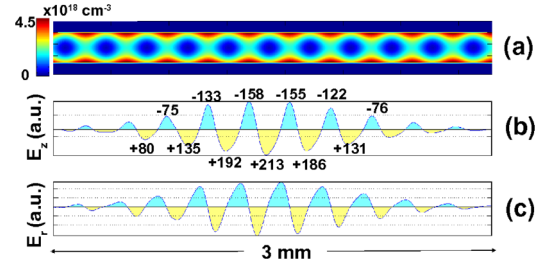


FIG. 2 (color online). We approximate the plasma waveguide shown in Fig. 1(b) with (a) a simple electron density profile to model laser pulse propagation and electron acceleration. FDTD simulation results show accelerating (b) and focusing (c) forces felt by a properly phased relativistic ($v = c$) electron copropagating with a femtosecond laser pulse. Several acceleration and deceleration half-dephasing cycles in (b) are labeled to show the work done on the electron in that region, with acceleration clearly dominating. The focusing force (c) is similarly QPM'd for this electron, to a lesser degree.

The transverse electric field shown in 2(c) is similarly QPM'd, which contributes to a net radial focusing or defocusing force. The laser group velocity is subluminal; the electron starts behind the laser pulse and overtakes it. This “pulse length dephasing” limits the interaction length. Leakage of the laser pulse out of the waveguide is minimal, and plasma dispersion does not interfere with acceleration.

Starting from these encouraging results, we introduce an analytic model neglecting leakage and dispersion (which are less pronounced for a shorter wavelength) in order to study more realistic parameters. We start with the radial component of the laser vector potential:

$$A_r = \hat{A}_r(r, z, t) \exp[i(k_0 z - \omega_0 t)] + \text{c.c.} \quad (1)$$

where k_0 and ω_0 are the central wave number and frequency of the laser pulse, respectively, and $\hat{A}_r(r, z, t)$ is a slowly varying envelope. We assume the pulse is azimuthally symmetric and consider plasma channels with low electron densities such that the plasma frequency satisfies $\omega_p \ll \omega_0$. In this regime, the envelope \hat{A}_r evolves on a time scale much longer than the laser period. The slowly varying envelope equation then determines the evolution of the laser pulse:

$$\left[2ik_0 \left(\frac{\partial}{\partial z} + \frac{1}{c} \frac{\partial}{\partial t} \right) + \frac{1}{r} \frac{\partial}{\partial r} r \frac{\partial}{\partial r} - \frac{1}{r^2} \right] \hat{A}_r = \frac{\omega_p^2(r, z)}{c^2} \hat{A}_r \quad (2)$$

where $\omega_0 = k_0 c$, and we have assumed that the electron plasma responds as a linear nonrelativistic cold fluid. Because the laser-electron dephasing length L_d depends on the electron's velocity [10], acceleration of subrelativistic electrons would require a structure with a graded modulation period to ensure L_d remains matched to the modulations over the entire interaction length. For mathematical simplicity, we consider a fixed modulation period,

suit to acceleration of electrons with $\gamma \gg 1$. We limit our analysis to a periodic electron density profile that models Fig. 2(a), $N_e(r, z) = N_0(1 + \delta \sin(k_m z)) + N_0'' r^2/2$, where δ is the relative amplitude of the density modulation, N_0'' determines the radial dependence, and k_m is the wave number describing the axial periodicity of the channel. Exact solutions to Eq. (2) which satisfy appropriate boundary conditions exist for this profile, which simplifies analysis of electron beam dynamics. Once A_r has been determined, A_z and the axial electric field can be determined by $\vec{\nabla} \cdot \vec{A} \approx 0$, which is consistent with $\omega_p \ll \omega_0$. The slowly varying envelope approximation neglects second derivatives in z and t in the wave equation which are responsible for subluminal group velocity, but the group velocity can be explicitly restored by replacing $c^{-1} \partial/\partial t$ with $v_g^{-1} \partial/\partial t$ in Eq. (2). Here, $v_g = 1 - \omega_{p,0}^2/2\omega^2 - 4/(k_0 w_{\text{ch}})^2$, and we define $\omega_{p,0}^2 = \langle \omega_p^2(0, z) \rangle_z$, where the brackets represent an average over z . Assuming Gaussian temporal dependence, the lowest eigenmode solution of Eq. (2) is

$$\hat{A}_r(r, z, t) = A_0 \frac{r}{w_{\text{ch}}} e^{-r^2/w_{\text{ch}}^2 - (z - v_g t)^2/\sigma_z^2} \times \sum_n i^n J_n(\psi) e^{-i\psi + i(\delta k + n k_m)z} \quad (3)$$

where $J_n(\psi)$ is the n th order Bessel function, $\psi = \delta \omega_{p,0}^2/2c^2 k_0 k_m$, and $\delta k = -k_0^{-1}(\omega_{p,0}^2/2c^2 + 4/w_{\text{ch}}^2)$. This is a sum of axial spatial harmonics of relative amplitude $J_n(\psi)$.

Matching the corrugation period to L_d is equivalent to matching the phase velocity of a spatial harmonic to the electron velocity. The effective phase velocity $v_{p,n}$ for the n th harmonic is $v_{p,n}/c = 1 - n k_m/k_0 + \omega_{p,0}^2/2\omega^2 + 4/(k_0 w_{\text{ch}})^2$, where an appropriate choice of n and k_m gives a ‘‘slow wave’’ harmonic ($v_p < c$) necessary for electron acceleration.

To determine a scaling law for direct electron acceleration, we consider an electron with initial conditions $(r, v_r) = (0, 0)$, and $(z, v_z) = (z_0, v_{z,0})$, where $v_{z,0}$ is assumed to be close enough to c such that the electron remains in the accelerating phase of the QPM field over the process of acceleration. For our experimental conditions of $(\omega_{p,0}/\omega_0)^2(k_0/k_m) \ll 1$ [7,8], $\psi \ll 1$ and $J_n(\psi) \sim \psi^n/2^n n!$. The amplitude of the harmonics decreases quickly with n , so we focus on $n = 1$ and set $v_{p,1} = v_{z,0}$. Choosing z_0 to optimize acceleration and integrating the axial electric field over the pulse length dephasing time $\sigma_z/(v_g - v_{z,0})$ using $v_{z,0} \approx c$, we obtain for the energy gain

$$\frac{\Delta E}{m_e c^2} \Big|_{\text{DA}} \sim 4\delta a_0 \left(\frac{\sigma_z}{w_{\text{ch}}}\right) \left(\frac{\lambda_p}{\lambda}\right)^2 \left(1 + \frac{2\lambda_p^2}{\pi^2 w_{\text{ch}}^2}\right)^{-2} \quad (4)$$

where $\lambda_p = 2\pi c/\omega_{p,0}$. The pulse length dephasing time limits the interaction length. By comparison, the

dephasing-limited energy gain for resonant laser-wakefield acceleration is [13]

$$\frac{\Delta E}{m_e c^2} \Big|_{\text{WF}} \sim \frac{a_0^2}{(1 + a_0^2/2)^{1/2}} \left(\frac{\lambda_p}{\lambda}\right)^2 \left(1 + \frac{\lambda_p^2}{\pi^2 w_{\text{ch}}^2}\right)^{-1}. \quad (5)$$

For a wavelength $\lambda = 800$ nm, matched beam radius $w_{\text{ch}} = 15$ μm , normalized amplitude $a_0 = 0.25$ corresponding to a laser power of 1.9 TW, pulse length $\sigma_z/c = 300$ fs, on axis plasma density $N_0 = 7 \times 10^{18}$ cm^{-3} , corrugation amplitude $\delta = 0.9$, and modulation period of $T_m = 349$ μm (we use these parameters in our following calculations), we have $\Delta E/mc^2|_{\text{DA}} \sim 1000$. In [13], a 7.16 TW, 100 fs pulse in a suitable plasma channel gives $\Delta E/mc^2|_{\text{WF}} \sim 750$, a slightly reduced acceleration with similar pulse energy. However, it is with smaller lasers that direct acceleration (a linear process) has its strongest advantage: replacing 1.9 TW with 30 GW would still give $\Delta E/mc^2|_{\text{DA}} \sim 125$, whereas (extremely nonlinear) wakefield acceleration is inoperable with such small lasers.

To study electron beam dynamics, we integrate the relativistic electron equations of motion in the laser electromagnetic field determined by Eqs. (1) and (3). We neglect space-charge effects, which become important when the axial electric field due to the bunched beam current becomes comparable to the QPM accelerating field. We estimate this gives an upper limit on the beam current of $I_{\text{max}}[A] < 1.7 \times 10^4 a_0 J_1(\psi) w_{\text{ch}}/\lambda$, which for our parameters is $3 \times 10^4 A$, or 40 pC per microbunch.

Figures 3(a) and 3(b) show maximum particle energy gain versus time. The pulse length dephasing time for this simulation is 130 ps. In Fig. 3(a), the effective phase velocity of the $n = 1$ harmonic is matched to three different initial electron velocities by tuning the modulation period, which could be accomplished experimentally by inserting imaging optics in the channel formation beam shown in Fig. 1 [7]. In Fig. 3(b), the phase velocity of the $n = 1$ harmonic was set to c for all three initial electron energies. The lines labeled ‘‘scaling’’ give the maximum energy gain based on the amplitude of the $n = 1$ component. Clearly, it is better to have electrons ‘‘catch up’’ to a slightly faster wave than for them to be initially resonant with but eventually overtake a slower one.

An electron displaced from the axis will experience two types of transverse force. The first type is a QPM focusing or defocusing due to the slow wave spatial harmonic. For an electron near the peak of the pulse and slightly off axis ($r \ll w_{\text{ch}}$), this force is

$$F_r^{\text{sw}} = \frac{m_e c^2 k_0 \delta a_0}{1 + 2\lambda_p^2/(\pi^2 w_{\text{ch}}^2)} \frac{r}{w_{\text{ch}}} \left[1 - \frac{v_z}{c} \left(1 + \frac{8}{k_0^2 w_{\text{ch}}^2} \right) \right] \times \cos(k_0 z - \omega t). \quad (6)$$

For electrons distributed uniformly over several wavelengths in z , equal numbers will experience focusing and defocusing from the QPM fields. The QPM radial force is

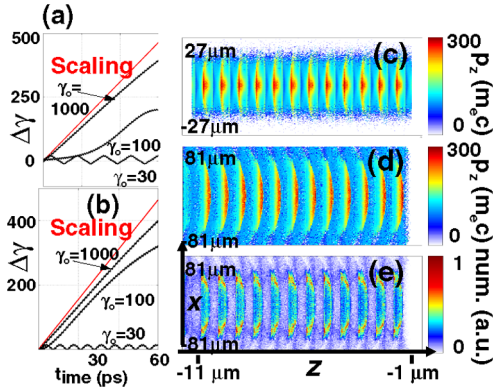


FIG. 3 (color online). (a) Energy gain vs time with the slow wave phase velocity matched to the initial electron velocity, and (b) the slow wave velocity is set to c . Allowing the electrons to catch up to the slow wave velocity reduces the dephasing due to acceleration at higher energies. (c) Average final z momentum as a function of initial position (z_0, x_0). (d) Average final z momentum as a function of final position (z_f, x_f) relative to the leading electron. (e) Final electron density as a function of final position (z_f, x_f). The electron beam has become bunched and focused.

90° out of phase with the corresponding axial force, so the focusing and defocusing force vanishes for particles in the maximum accelerating phase. The second force is the ponderomotive force on the electrons from the $n = 0$ fundamental laser mode:

$$F_r^{\text{pm}} = -\frac{2mc^2}{\gamma_0} \frac{r}{w_{\text{ch}}^2} |a_0|^2 \times \left[1 - \frac{4}{\pi^2} \frac{v_z}{c} \left(\frac{\lambda_p}{w_{\text{ch}}} \right)^2 \left(1 + \frac{\lambda_p^2}{\pi^2 w_{\text{ch}}^2} \right)^{-1} \right]^2 \quad (7)$$

which is obtained by linearizing the equations of motion about $v_z = v_{z,0}$ and averaging over the fast time scale $k_m v_z$. Because the mode fields peak off axis, this force focuses regardless of initial electron phase. Generally, the peak QPM force exceeds the ponderomotive force, except in the maximum accelerating phase for which the radial QPM force vanishes. To examine transverse dynamics, we distribute electrons uniformly in z from $1 \mu\text{m}$ to $11 \mu\text{m}$ behind the pulse maximum and with a Gaussian distribution in r with width σ_r . Figures 3(c) and 3(d) show the number-averaged final z momentum as a function of initial and final position, respectively, for an initial electron beam radius of $9 \mu\text{m}$. Efficiency is very injector-dependent: to be accelerated, electrons must start in “buckets” one half of a slow wavelength long and less than one laser spot size wide; for our parameters, the space charge limit per bucket is <40 pC. Figure 3(e) shows the final electron beam density as a function of position; the beam has acquired a significant transverse spread which peaks off axis.

Comparing Figs. 3(d) and 3(e), we see that these peaks are mostly composed of lower energy electrons that have been expelled from the center of the buckets. All these effects can be clearly seen in a multimedia file [14], which shows the time evolution of a subset of the particles from Figs. 3(c) and 3(d) in a window moving to the right at $\gamma = 100$. QPM focusing and defocusing buckets, accelerating and decelerating buckets, and slow electron dephasing/rephasing are all evident. The particle bunch is longer than one accelerating “bucket”; some electrons are decelerated and some are defocused. Electrons that do not accelerate slip into a defocusing region and are ejected from the waveguide. The highest-energy electrons simply plow ahead while absorbing energy, largely unaffected by transverse forces, and gain 151 MeV over 1.8 cm, a gradient of 84 MeV/cm. A 40 pC bucket would absorb about 6 mJ of energy, $\sim 1\%$ of the driving pulse, while the number of loaded buckets depends on the injector. Since this acceleration process is linear and scales with the square root of laser power, a laser power of only 30 GW would give a respectable gradient of 10.6 MV/cm. Further details of the calculation presented here can be found in Ref. [15].

This work was supported by the U.S. Department of Energy and the National Science Foundation.

*Andrew.G.York+prl@gmail.com

- [1] T. Tajima and J.M. Dawson, Phys. Rev. Lett. **43**, 267 (1979); E. Esarey *et al.*, IEEE Trans. Plasma Sci. **24**, 252 (1996); V. Malka *et al.*, Science **298**, 1596 (2002).
- [2] *Laser Acceleration of Particles*, edited by P. J. Channell, AIP Conf. Proc. No. 91 (AIP, New York, 1982).
- [3] <http://www2.slac.stanford.edu/vvc/accelerators/structure.html>.
- [4] W.D. Kimura *et al.*, Phys. Rev. Lett. **74**, 546 (1995).
- [5] T. Plettner, R.L. Byer, E. Colby, and B. Cowan *et al.*, Phys. Rev. Lett. **95**, 134801 (2005).
- [6] M.D. Perry and G. Mourou, Science **264**, 917 (1994).
- [7] B.D. Layer *et al.*, Phys. Rev. Lett. **99**, 035001 (2007).
- [8] T.R. Clark and H.M. Milchberg, Phys. Rev. E **61**, 1954 (2000).
- [9] P. Serafim, P. Sprangle, and B. Hafizi, IEEE Trans. Plasma Sci. **28**, 1155 (2000).
- [10] A. York, B.D. Layer, and H.M. Milchberg, in *Advanced Accelerator Concepts*, AIP Conf. Proc. No. 877 (AIP, Melville, New York, 2006), p. 807.
- [11] M. Xie, Report No. LBNL-48236, 2001.
- [12] A. Farjadpour *et al.*, Opt. Lett. **31**, 2972 (2006).
- [13] R.F. Hubbard *et al.*, IEEE Trans. Plasma Sci. **28**, 1159 (2000).
- [14] <http://www.glue.umd.edu/~york/scat.mpg>.
- [15] J.P. Palastro, T.M. Antonsen, S. Morshed, A.G. York, and H.M. Milchberg, Phys. Rev. E **77**, 036405 (2008).